coatings

MDPI

Article

Comparative Study Between Ammonium Phosphate and Ethyl Silicate Towards Conservation of Prehistoric Paintings in the Magura Cave (Bulgaria)

Enrico Sassoni [1,2,*], Elisa Franzoni [1,2], Milyana Stefanova [3], Zdravko Kamenarov [3], Paolo Scopece [4] and Emanuele Verga Falzacappa [4]

1 Department of Civil, Chemical, Environmental and Materials Engineering (DICAM), University of Bologna, Via Terracini 28, 40131 Bologna, Italy; elisa.franzoni@unibo.it
2 Centre for Applied Research on Buildings and Construction (CIRI-EC), University of Bologna, Via del Lazzaretto 15/5, 40131 Bologna, Italy
3 NTConservation ltd, Blv. Al. Konstantinov 51, 1504 Sofia, Bulgaria; milyana13@yahoo.com (M.S.); kamenarov_zdravko@abv.bg (Z.K.)
4 Nadir srl Plasma & Polymers, Via Torino 155/b, 30172 Venezia, Italy; scopece@nadir-tech.it (P.S.); falzacappa@nadir-tech.it (E.V.F.)
* Correspondence: enrico.sassoni2@unibo.it; Tel.: +39-051-2090-429

Received: 16 January 2020; Accepted: 6 March 2020; Published: 9 March 2020

Abstract: This study aimed at evaluating the effectiveness and the compatibility of two alternative treatments, in view of their possible use for conservation of prehistoric paintings in the Magura cave (Bulgaria). The paintings are made of bat guano applied over limestone; therefore, two sets of laboratory specimens were considered: stone specimens and stone specimens covered with a layer of sterilized bat guano. The two investigated treatments were a commercial product based on ethyl silicate ("ES") and a solution of diammonium hydrogen phosphate ("DAP"), aimed at forming calcium phosphates. The results of the study indicated that both treatments were able to increase the mechanical properties of stone, the increase being higher for "DAP". Both consolidants caused acceptable color changes, but the "ES" treatment significantly decreased stone wettability, water absorption, and water vapor permeability, while the "DAP" treatment slightly affected those properties. In the stone + guano specimens, the presence of the guano layer affected the penetration of the consolidants, thus partly reducing their effectiveness. Compared to the stone samples, the guano layer experienced a more intense color change, alongside visible cracking. However, the adopted methodology to replicate the cave paintings was not completely successful, as the so-deposited guano layer was very prone to detachment when dry, unlike cave paintings. Future work will be dedicated to assessing the consolidant performance onto samples that resemble even more closely the conditions of the cave paintings, by improving the methodology for the guano layer deposition and by contaminating specimens with soluble salts before consolidant application.

Keywords: cave painting; inorganic consolidant; hydroxyapatite; calcium phosphate; ammonium phosphate; ethyl silicate; TEOS; non-thermal plasma; wettability

1. Introduction

The present paper aimed at investigating the effectiveness and the compatibility of two treatments that have been taken into consideration for the conservation of prehistoric paintings in the Magura cave (northwest Bulgaria). The Magura cave contains impressive prehistoric paintings, displaying both figurative and abstract compositions [1]. Religious ceremonies, hunting scenes, signs, and graphic motifs decorate one of the cave chambers—the Gallery with the paintings (Figure 1).

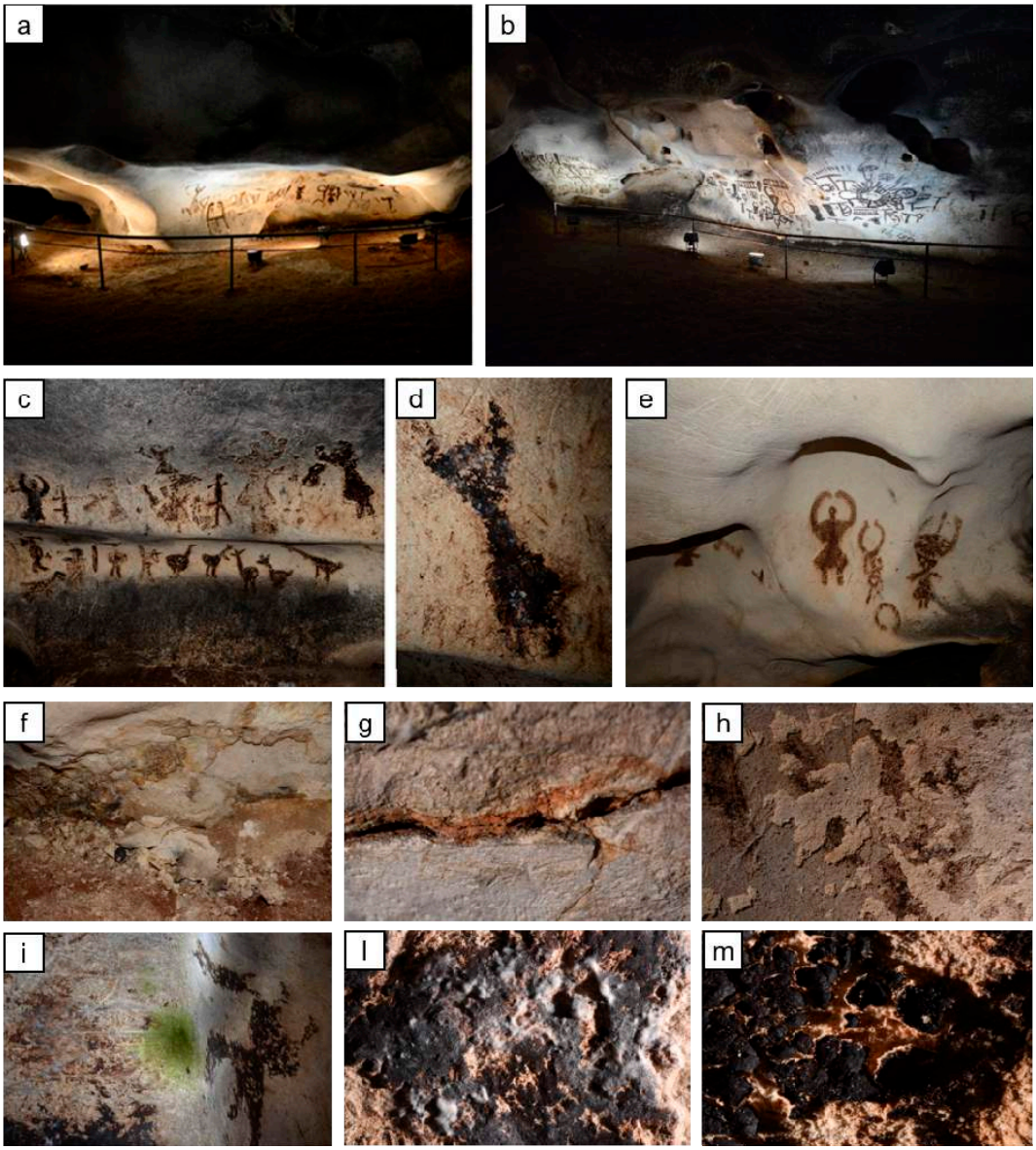

Figure 1. General view of the Gallery with the paintings in the Magura cave (Bulgaria) (**a**,**b**), details of the cave paintings (**c**,**d**,**e**), and details of the deterioration patterns ((**f**,**g**,**h**)—cracks, powdering, blistering, and fragmentation of the limestone; (**i**,**l**)—biological colonization; (**m**)—cracking and loss of the original guano painting due to the drying of the surface and powdering of the stone).

These artworks, dating back to some 5500 years ago, are made of fossilized guano of cave-dwelling bats applied over limestone [2–5]. After opening to the public in 1961, with the consequent presence of visitors and the use of artificial light, the delicate balance of environmental conditions inside the cave has been altered. Despite the cultural relevance of the Magura Cave, unfortunately, the micro-environmental data, such as temperature, relative humidity, CO_2 concentration, and atmospheric pressure, have never been professionally measured and controlled. Today, the cave suffers from biological colonization and stone pulverization, originated by crystallization of soluble salts present in rising damp from the ground. Deterioration patterns, such as green biofilm and white and black colorations over the stone/paintings surface, together with limestone powdering, blistering, and fragmentation [6] (Figure 1), led to the closure of the Gallery in May 2019.

The preservation of the cave paintings requires challenging interventions to face the growth of bio-organisms and the deterioration of the stone. As for biological growth, the use of biocides is

dangerous because they may completely alter the balance of microbial communities in the cave with negative consequences [7]. For this reason, biodeactivation by non-thermal plasma sterilization has been attempted, and some encouraging results have been obtained [8]. As for stone consolidation, the issue is particularly challenging for the following reasons:

(1) the presence of the guano layer creating the paintings. The case of the Magura cave is different from the case of wall paintings [9] and also from the case of other prehistoric paintings, such as those in the Altamira [10] and Lascaux [11] caves. In the wall paintings, the pigments were dispersed in limewater and then applied directly onto the wet plaster (in the so-called "fresco" technique) and/or they were applied onto the dried plaster by using an organic binder, such as egg, milk, or vegetal extractives [9]. In the case of other prehistoric paintings, the pigments, usually red (Fe_2O_3), black (charcoal, soot, bone charcoal, or Mn oxides), and more rarely yellow (FeOOH) and brown (ochres), were mixed with an extender and/or a binder [10,11]. The case of the Magura cave, with paintings laid on the cave walls by bat guano having a plastic consistency similar to clay [5], is substantially different from the situations discussed above, with only a few similar cases, such as the Baylovo Cave in Bulgaria and the "Grotta dei Cervi" (Deer cave) in Italy [7]. To our knowledge, no case of consolidation of cave paintings made of bat guano has been reported in the scientific literature.

(2) the presence of soluble salts inside the stone pores. This is an issue for two reasons: (i) salts already present inside the pores may lead to failure of the consolidation intervention, if the tip of the cracks among grains is filled with salts, so that no effective sealing of the crack tip can be achieved by the consolidant [12]. To prevent this, it is usually recommended that salts be extracted by poulticing before consolidants are applied, but this is useless in the present case, as salts are continuously supplied from the ground; (ii) salt crystallization cycles taking place after stone consolidation may lead to stress at the grain boundaries, with possible failure of the consolidation intervention if the stone tensile strength is exceeded. Experiences of application of various consolidants onto salt-laden stones, possibly later subjected to further salt crystallization cycles, have been reported in the literature, as detailed in the following.

(3) the environmental conditions in the cave. Because of its hypogeous nature, the temperature in the cave ranges between 12 and 25 °C, while the relative humidity (RH) is constantly in the range 65–90%. Such environmental conditions may have an impact on a consolidant performance, as discussed below.

In these conditions, the selection of consolidants to be tested and possibly applied in the Magura cave is very hard, as none of the commercially available treatment seems ideal for application onto the limestone and the paintings in the cave. The two consolidants tested in this study, namely, a commercial product based on ethyl silicate and diammonium hydrogen phosphate, were selected based on the following reasoning.

Organic consolidants, such as acrylic resins, were discarded because, in the past, the use of polymeric treatments often led to enhanced deterioration to such an extent that removal of polymers applied in the past is nowadays one of the greatest issues in materials science for cultural heritage conservation [13]. The failure of organic consolidants often originates from water vapor being impeded to move from the interior of the consolidated substrate towards the exterior [14]. This risk would be particularly high in the case of the Magura cave, where water is continuously supplied from the ground, and systems currently used in building for damp reduction are not applicable.

Among inorganic treatments, nanolimes were first considered because of their good chemical-mineralogical compatibility with limestone and because they have shown a good performance when applied onto lime-based frescoes and wall paintings [9,13–16]. However, as already mentioned, a substantial difference exists between wall paintings and paintings in the Magura cave, made of bat guano. Moreover, in the case of the Magura cave, the purpose was the consolidation of the powdering stone with the bat guano painting on the surface, and not of the painting layer alone;

therefore, a consolidant able to penetrate in depth in the substrate was needed. In several cases of application of nanolimes onto stones, a poor penetration depth (<1 mm) has been reported [14]. Nanolime accumulation below the surface is likely not due to nanoparticle coagulation preventing penetration, but rather to nanoparticle re-transport towards the surface during drying [14]. When applied onto the salt-laden stone, conflicting results have been reported about the ability of nanolimes to increase stone durability to salt weathering [17,18]. In fact, in some cases, nanolimes have been reported to increase the crystallization pressure in the treated stone, as a result of the alteration in pore size distribution after consolidation, with a consequent decrease in durability [17]. Considering the limitations exhibited by nanolimes in terms of penetration depth and durability to salt weathering, which are both very important aspects for the conservation of the Magura cave limestone and paintings, nanolimes were discarded, and further options were explored.

Ammonium oxalate was considered as this treatment was specifically developed for the protection and consolidation of carbonate substrates, like wall paintings, marble, and limestone [19]. A positive aspect of the ammonium oxalate treatment is that encouraging results have been reported in the literature about its application onto salt-laden stones [20,21]. Removal of salts before application of ammonium oxalate solutions was found to be not as crucial as in the case of organic treatments because ammonium oxalate does not completely occlude pores (although forming a surface coating) [20]. However, ammonium oxalate was finally discarded because of its reduced availability in the market. The method based on barium hydroxide [19] was discarded as well due to its recommended poultice application (aimed at reducing the risk of surface whitening) and its possible reaction with nitrate salts (giving barium nitrate, a very damaging salt upon crystallization). Given the impossibility to apply the consolidant in the cave by poultice and the presence of several salts in the stone, barium hydroxide was not considered for the present application.

Ammonium phosphate was proposed years ago as an improvement of the ammonium oxalate treatment for the consolidation and protection of carbonate stones [22,23]. The treatment is based on the formation of new calcium phosphates (ideally hydroxyapatite, the least soluble calcium phosphate at pH > 4 [24]) from the reaction between an aqueous solution of ammonium phosphate and the stone [22]. This reaction occurs in 24–48 h during which the stone is kept impregnated with the ammonium phosphate solution; therefore, the environmental conditions of the cave are not expected to negatively affect the treatment success. Thanks to the low viscosity of the phosphate solution and to the absence of nanoparticles, a good penetration depth is usually achieved (>5 cm in highly porous limestone) [25]. So far, the treatment has provided good results on a variety of substrates [25], including many types of natural stones [26–32], mortars [33,34], and stuccoes [35]. Recently, the interaction between ammonium phosphate solutions and pigments used in wall paintings has been investigated, and, in most of the cases (but not in all), the treatment has been found to cause negligible color changes [36]. This is encouraging towards the use of this treatment for the conservation of wall paintings, even though the substantial difference of the Magura cave paintings remains. Another positive aspect of the ammonium phosphate treatment is that the presence of salts in the stone pores has proven to be not detrimental for the treatment success [30,37], but, of course, this depends on the amount and type of salts and on the features of the stone pore system. Moreover, accelerated durability tests have shown that ammonium phosphate treatment is able to increase the durability of treated stone to salt crystallization cycles [38–40]. Furthermore, considering the presence of hydroxyapatite in the Magura cave limestone (although not in the limestone used for the laboratory tests), the chemical-compatibility of the ammonium phosphate treatment can be considered as excellent. For all these reasons, the phosphate treatment was regarded as highly promising for application in the Magura cave and hence was investigated in this study. As described in Section 2.3.2, two alternative formulations of the phosphate treatment were initially considered, and, after some preliminary screening tests, the most promising one was chosen.

Considering that ammonium phosphate has the limitation that experience on its use dates back only to a few years ago and that only a limited number of applications onto real case studies have been reported, a possible alternative consolidant was searched. Products based on ethyl silicate were

taken into consideration as they are known to generally exhibit a good penetration depth into porous substrates [41], often sensibly higher than that of nanolimes [14]. One major limitation of ethyl silicate when applied onto carbonate stones, as would be the case in the Magura cave, is that its consolidating effectiveness is lower than in the case of silicate stones. In fact, in the latter case, chemical bonding can take place between the silicate substrate and the silica gel resulting from hydrolysis-condensation of ethyl silicate, while, in the case of carbonate stones, only physical bonding can occur [12]. Nonetheless, significant increases in mechanical properties of carbonate stones treated by ethyl silicate have been reported [42], especially when the stone contains even limited quarzitic fractions that may allow for some chemical bonding between the consolidant and the substrate [43]. To improve the performance of ethyl silicate onto carbonate stones, several routes have been investigated, such as the use of coupling agents [41] or the addition of organic molecules (e.g., polyethylene glycol chains end-capped with carboxylic acid groups [44]) or inorganic nanoparticles (e.g., amorphous calcium carbonate and amorphous calcium oxalate [45]) directly into the ethyl silicate solution. Cases of application of ethyl silicate products onto salt-laden stones have been reported in the literature, with mixed results [18,37,41,46], also due to the variable nature of the ethyl silicate products in the market in terms of oligomer size, solvent nature, catalyst, etc. When salts are present in the pores of the treated stone, the consolidating effectiveness is not dramatically diminished [18,37]. However, the alterations induced by ethyl silicate in the stone pore size distribution may increase the salt crystallization pressure, thus decreasing the resistance to salt crystallization cycles, as assessed on both initially salt-contaminated [18] and uncontaminated [38,39] stone. In comparative studies, the salt resistance of carbonate stones treated by ethyl silicate proved to be lower compared to ammonium phosphate (but still higher than untreated stone) [38,39]. Another import factor when evaluating the suitability of ethyl silicate for the case of the Magura cave is the temporary hydrophobicity induced by ethyl silicate [12]. In fact, until hydrolysis-condensation reactions are completed, the treated stone remains hydrophobic because of the presence of residual ethoxy groups [12]. Completion of hydrolysis-condensation reactions can take as long as 6–7 months [12,47,48], even though the technical data sheet of commercial products usually report that the product reaction is completed in 1 month. The hydrophobic behavior of stone treated by ethyl silicate, which generally preserves permeability to water vapor but prevents the transport of liquid water through the consolidated layer, may be an issue in the case of Magura cave, where rising damp from the ground is present. On the other hand, the high relative humidity (65–90%) inside the cave is expected to speed up the hydrolysis-condensation reactions, which is positive. To accelerate the curing of ethyl silicate, thus re-establishing a hydrophilic behavior in a shorter time, various methods have been proposed, which basically consist of supplying water [47] or water-ethanol mixtures [48] to promote hydrolysis reactions. However, such methods seem unfeasible in the case of the Magura cave, as they involve the application of a poultice onto the treated surface, which may lead to damage and detachment of the cave paintings. All things considered, even though not ideal, ethyl silicate was regarded as worthy of investigation as a possible alternative to ammonium phosphate. Among the numerous products available in the market, a commercial formulation enhanced with antimicrobial ability was used, as described in detail in Section 2.3.1.

For testing the two selected consolidants, the complex situation of the Magura cave had to be necessarily simplified, to isolate variables and better evaluate the consolidant performance. With regard to the three aspects discussed above, the following decisions were made:

(1) To evaluate the effects of the two consolidants not only on limestone but also on the cave paintings, two types of laboratory specimens were considered: (i) specimens made of a limestone similar to that in the cave and (ii) specimens made of the same limestone with a layer of sterilized bat guano deposited on top, to resemble the prehistoric paintings in the cave. The procedure for the deposition of the guano layer, described in detail in Section 2.2, was developed in such a way to likely resemble the process of creation of the paintings, even though, of course, freshly prepared samples could not be identical to cave paintings that have undergone about 5500 years of fossilization.

(2) To evaluate the effects of the two consolidants onto salt-laden samples, to be further subjected to salt crystallization cycles after consolidation, would have been ideal. However, this would have made the evaluation of the consolidants on the two types of specimens (stone and stone+guano) even more difficult, with the risk that the influence of salts in the pore and the guano layer on the stone surface could be hard to distinguish. For this reason, at the present stage of the research, the consolidants were applied onto uncontaminated specimens, which were used to evaluate the effectiveness and the compatibility of the treatments in these simplified conditions. Application onto salt-laden samples, together with the evaluation of the durability of the consolidated substrates, was left to a future stage of the research, once the performance on this simplified system has been assessed.

(3) At this stage of the research, the effects of the treatments were evaluated in laboratory conditions (T = 19–23 °C, RH = 45–55%), which were regarded as conservative with respect to the environmental conditions in the cave (T = 12–25 °C, RH = 65–90%). In fact, the higher relative humidity in the cave was expected to positively influence the rate of hydrolysis-condensation reactions of ethyl silicate (while no effect was expected on the reaction of the ammonium phosphate treatment). Nonetheless, to obtain some preliminary information on the performance of two consolidants in the real environmental conditions, specimens treated with the two consolidants were exposed in the Magura cave for 9 months, as described in detail in the following.

In the frame of the experimental choices described above, in the present paper, the performance of the two consolidants was characterized in terms of effectiveness (penetration depth, dynamic elastic modulus, and resistance to abrasion) and compatibility (alterations in color, pore size distribution, contact angle, water sorptivity, water absorption, water vapor permeability). The results obtained in the present study will be used in future research to evaluate also the durability of the two treatments, also in salt-contaminated stone.

2. Materials and Methods

2.1. Stone Specimens

Two small samples of the Magura cave limestone were available for characterization, namely, a stone piece affected by severe powdering and a hard surface crust. Although not sufficient to fully characterize the stone in the cave, these samples were characterized to select a stone for laboratory testing that could suitably resemble the limestone in the cave. The minerals present in the two samples were determined by powder X-ray diffraction (XRD), using a Philips diffractometer (Milan, Italy) with PW1830 generator and PW1820 goniometer (40 kV and 30 mA, 2θ range 3°–80°, step size 0.025 2θ, time per step 1 s). Additional minerals, present in quantities below the sensitivity of XRD, were investigated by Fourier transform infrared spectrometry (FT-IR), using a Perkin Elmer Spectrum Two spectrometer (Milan, Italy) (ATR mode, 2000–400 cm^{-1} range, spectral resolution 2 cm^{-1}, 32 scans, data interval 1 cm^{-1}). The amount of calcite in the samples was quantified by Dietrich–Frühling gas volumetric method, i.e., by measuring the CO_2 volume released by reacting the powdered sample with HCl. The open porosity of the samples was assessed by mercury intrusion porosimetry (MIP), using a Pascal 140 and 240 instrument. The Magura cave limestone was found to be mainly composed of calcite (the only mineral detected by XRD), quantified as 90.0 ± 1.8 wt.% (by gas volumetric method). Based on FT-IR, the remaining fraction was composed of hydroxyapatite and possibly traces of quartz. In terms of microstructure, the open porosity was found to range significantly between the two samples, from 2% for the hard crust to almost 48% for the powdering sample.

The stone selected for the laboratory tests was Vratsa limestone, which is quarried very close to the Magura cave (Oreshets quarry, Municipality of Vidin, Bulgaria, 20 km from the cave). In terms of mineralogical composition (assessed as above), Vratsa limestone was mainly composed of calcite (80.0 ± 0.1 wt.%), the remaining fraction being quartz (the only other phase detected by XRD and FT-IR). The open porosity of Vratsa limestone (assessed as above) exhibited some variability, ranging

from 11% to 18%. Although not identical to the cave limestone, the Vratsa limestone was considered as still suitable, as it exhibited mineralogical composition similar to the Magura cave limestone (although the minor phases were different) and open porosity that was intermediate between the values registered for the samples from the cave (which, however, were very different from each other).

Specimens of Vratsa limestone to be used for the tests (labeled "ST") were sawn in the form of prisms ($7 \times 7 \times 3$ cm^3) and cubes (5 cm side).

2.2. Stone+Guano Specimens

To resemble the cave paintings, the original guano from the Gallery with the paintings, which is home of 8 different bat species, was used. The guano has an organic matter content greater than 40%, visible chitinous insect remains and is a favorable environment for many different types of microorganisms [49,50]. For safety reasons, the original bat guano was exposed to autoclave sterilization (Laboratory of Geological Microbiology, Department of Microbiology, Sofia University St. Kliment Ohridski, Bulgaria).

The stone+guano specimens (labeled "ST+G") were prepared, starting from the "ST" specimens, by depositing a layer of sterilized bat guano on top, following the procedure illustrated in Figure 2. First, a small amount of guano was added with deionized water so as to reach a suitable consistency (guano:water ratio of 1:2 by weight). After mixing the guano with water, the obtained mixture was applied onto one face of the specimens by brush. After about 2 min, the second layer of guano was applied in the same way.

Considering that the so-deposited guano layer becomes dusty and starts to detach from the substrate when it dries, the consolidant application was carried out 30 min after the guano application to avoid the stone+guano specimens from becoming too powdery.

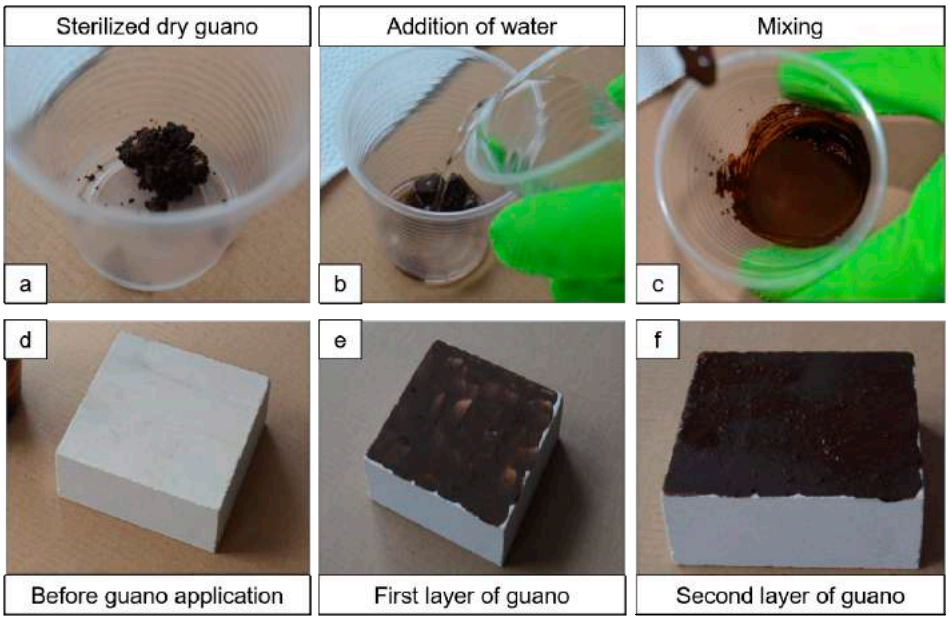

Figure 2. Procedure for guano application: sterilized dry guano (**a**) is added with water (**b**); after mixing (**c**), stone specimens (**d**) are covered with the first layer of guano (**e**) applied by brush; after about 2 min, the second layer of guano (**f**) is applied.

2.3. Consolidants

The two consolidants selected for testing were a commercial product based on ethyl silicate (labeled "ES") and diammonium hydrogen phosphate (labeled "DAP"). In both cases, the consolidants were applied by brushing onto one face of the specimens (the face already covered with the guano

layer, in the case of the "ST+G" specimens). For each consolidant, 7 prismatic and 2 cubic specimens were treated.

2.3.1. Ethyl Silicate-Based Consolidant

The commercial product "Bio Estel New" by CTS Srl (Florence, Italy) was selected. According to the manufacturer's technical data sheet, "Bio Estel New" is based on ethyl silicate and isopropyl alcohol as a solvent, and it combines consolidating ability with protective ability against microorganisms. The technical data sheet also reports that the product is suitable for application onto silicate and carbonate stones, especially underwater stones and stones in a very humid environment, and that the product reaction is completed in about 4 weeks at T = 20 °C and RH = 40–50%.

The ES consolidant was applied by brushing until apparent refusal (7 brush strokes), waiting for the product to be absorbed between two consecutive brush strokes. At the end of the consolidant application, specimens were left to cure in laboratory conditions (T = 21 ± 2 °C, RH = 50% ± 5%) for at least 4 weeks before characterization.

2.3.2. Phosphate Consolidant

For the phosphate treatment, diammonium hydrogen phosphate (DAP, $(NH_4)_2HPO_4$), calcium chloride ($CaCl_2{\cdot}2H_2O$), and ethanol (EtOH), all purchased from Sigma-Aldrich (Milan, Italy, assay > 99%) were used. Based on results obtained in previous studies [22,25,51], two formulations of the phosphate treatment were initially considered for the tests: (i) 1 M DAP + 1 mM $CaCl_2$ and (ii) 0.1 M DAP + 0.1 mM $CaCl_2$ in 30 vol.% EtOH. Calcium chloride has the beneficial effect of accelerating the formation of calcium phosphates [51], while ethanol has been found to promote densification of the new calcium phosphates [52]. To identify the most promising treatment condition in the specific case of the specimens resembling paintings in the Magura cave, preliminary tests were carried on the "ST+G" specimens. The surface alteration following consolidant application, carried out 30 min after guano application, was visually evaluated. As illustrated in Figure 3, the formulation containing 0.1 M DAP + 0.1 mM $CaCl_2$ in 30 vol.% EtOH caused lower alteration (darkening and cracking) of the specimen surface, compared to the alternative formulation. Consequently, that formulation was selected and applied to the "ST" and "ST+G" specimens.

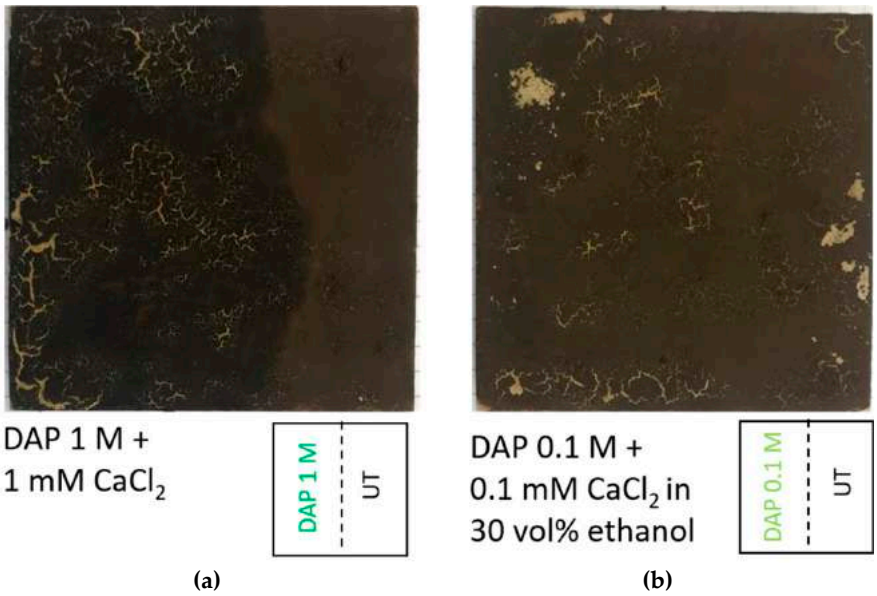

Figure 3. Alteration of the specimen surface caused by consolidant application 30 min after guano application: 1 M DAP + 1 mM $CaCl_2$ (**a**) and 0.1 M DAP + 0.1 mM $CaCl_2$ in 30 vol.% (**b**).

The "DAP" treatment was applied by brushing until apparent refusal (10 brush strokes), waiting for the product to be absorbed between two consecutive brush strokes. At the end of the consolidant application, specimens were wrapped in a plastic film to prevent evaporation and left to react for 48 h. Then, specimens were unwrapped, rinsed with deionized water (only in the case of the "ST" specimens), and left to dry at room temperature until constant weight.

2.4. Pre-treatment by Plasma

To evaluate whether penetration of the two consolidants into the stone might be enhanced, with a consequent improvement in the consolidating efficacy, part of the stone specimens was pre-treated by plasma, before consolidant application. Indeed, an improvement in wettability is a well-known effect of a wide range of plasma sources on different materials. Mainly, thanks to oxygen atoms implantation and the subsequent formation of polar groups on the treated surface, an increase in surface energy is typically observed together with a reduction in water contact angle [53].

To evaluate whether pre-treatment by plasma might be beneficial for the consolidant performance, right before consolidant application, part of the "ST" specimens was subjected to pre-treatment by plasma, carried out with a dual-frequency atmospheric plasma jet device (Stylus Plasma Noble provided by Nadir Srl, Venice, Italy) [54]. The following working parameters were adopted: 5 W power at 16 kHz, 30 W power at 27 MHz, argon gas flow as working gas at 10 L/min, and compressed air as cooling gas at 12 L/min. The 7×7 cm^2 surface of prismatic specimens were manually treated for a total exposure time of 2 min, maintaining a constant working distance of 3 mm between the plasma source and the specimen.

The effects of the plasma pre-treatment were evaluated in terms of static contact angle, amount of product absorbed, and increase in dynamic elastic modulus, assessed as described in the next paragraph.

2.5. Sample Characterization

The effectiveness and the compatibility of the two consolidants were investigated by comparing the properties of untreated ("UT") and treated specimens ("ES" and "DAP"), as described in the following.

2.5.1. Morphology of the New Phases

The morphology of the new phases formed over the treated surface was evaluated by observing samples (about $10 \times 10 \times 2$ mm^3, obtained by wet sawing from the prismatic specimens), using a field emission gun scanning electron microscope (FEG-SEM, Tescan Mira3, Brno, Czech Republic, WD = 10 mm, Voltage = 10 kV). Before SEM observation, the sample surface was made conductive by sputtering with aluminum.

2.5.2. Composition of the New Phases

The composition of the new phases formed over the treated surface was evaluated by analyzing powdered samples (obtained from the specimen surface using a spatula) by FT-IR, using the same instrument as in Section 2.1.

2.5.3. Penetration Depth

The penetration depth of the two consolidants into the "ST" and "ST+G" prismatic specimens was evaluated by fracturing them with a chisel to expose a cross-section, right at the end of the consolidant application (7 brush strokes in the case of ES, 10 in the case of DAP). The consolidant penetration depth was visually identified as the darker zone. Two replicate specimens were considered for each condition.

2.5.4. Dynamic Elastic Modulus

Dynamic elastic modulus (E_d) was measured on prismatic specimens, perpendicular and parallel to the plane of the slab (in the "ST+G" samples, perpendicular and parallel to the face covered with

guano). Given the absence of any clear anisotropy in the stone, values measured in the two directions parallel to the plane of the slab were averaged, so that, in the end, each specimen was characterized in terms of $E_{d\perp}$ and $E_{d//}$. E_d was calculated according to the formula $E_d = \rho \times v^2$, where ρ is the density and v is the ultrasonic pulse velocity. v was measured with a Matest instrument with 55 kHz transducers, using a rubber sheet to improve the contact between the transducers and the specimen. A rubber sheet instead of grease was used to improve the contact (as would be the standard procedure), in order not to stain the samples that later had to be consolidated. For instrument calibration, a standard bar with fixed traveling time was used. Five replicate specimens were tested.

2.5.5. Resistance to Abrasion

Resistance to abrasion was measured on prismatic specimens, in terms of material loss after an accelerated abrasion test, carried out following a previously developed method [55]. By partially modifying the PEI (Porcelain Enamel Institute) abrasion test, samples were tested by keeping steel spheres and corundum powder in rotatory motion over one of the 7×7 cm^2 faces of the specimens (the face already covered with the guano layer, in the case of the "ST+G" specimens), for a total of 15,000 rounds. The amount of material abraded during the test was then determined by comparing the sample weight before and after the test. Five replicate specimens were tested.

In the case of the "ST+G" samples, because guano flakes were prone to detach also from the area not directly subjected to the abrasion test, before the test all the guano-covered surface, not directly in contact with the steel spheres, was covered with scotch tape, so that no material loss could take place from that area.

2.5.6. Color Change

The color change after consolidation was measured on prismatic specimens by making use of a NH310 colorimeter. For the untreated and treated conditions, the LabCIE* color parameters (L^* = black–white, a^* = green–red, b^* = blue–yellow) were determined on duplicate specimens, repeating the measurements in three different spots for each specimen. For instrument calibration, a standard white sample supplied with the instrument was used. The color change (ΔE^*) between untreated and treated specimens was then calculated as $\Delta E^* = (\Delta L^{*2} + \Delta a^{*2} + \Delta b^{*2})^{1/2}$, considering the average L^*, a^*, and b^* values obtained for each condition.

2.5.7. Pore Size Distribution

The alterations in open porosity and pore size distribution following the treatments were determined by mercury intrusion porosimetry (MIP), using a Porosimeter 2000 by Carlo Erba (Milan, Italy) with Fisons Macropore Unit 120. MIP samples were obtained by chisel from prismatic specimens, always including the treated surface (where alterations were expected to be most pronounced). For each condition, two replicate samples were tested.

2.5.8. Static Contact Angle

For the untreated and treated conditions, the static contact angle was measured on prismatic specimens by making use of a DSA30 instrument by Krüss (Hamburg, Germany), calibrated according to its standard procedure. A drop of deionized water (4 µL volume) was released on the specimen surface, and then the drop profiles were recorded using a camera and analyzed by SCA20 software 1.0. The static contact angle was determined on duplicate specimens, repeating the measurements in three different spots for each specimen.

2.5.9. Water Sorptivity and Water Absorption

Water sorptivity (S) of untreated and treated specimens was measured on cubic specimens, according to the European Standard EN 15801 [56]. Deionized water was let penetrate the specimens

through the treated face, and the weight increase over time was periodically monitored. The amount of water absorbed by capillarity into the samples after 24 h (WA_{24h}) and 7 days (WA_{7d}) was determined. Two specimens were tested for each condition.

2.5.10. Water Vapor Permeability

The water vapor permeability of untreated and treated specimens was measured on prismatic samples and expressed in terms of water vapor diffusion resistance coefficient (μ), according to the European Standard EN 15803 [57]. A glass container was filled with a saturated aqueous solution of KNO_3 up to 3 cm from the top and the specimen was placed on top of the container, with the treated face towards the solution. The specimen was then glued to the container, and the lateral sides of the samples were sealed. The coefficient μ was calculated as $\mu = \delta_a/\delta_p$, where δ_a is the water vapor permeability of air, and δ_p is the water vapor permeability of the specimen. Two specimens were tested for each condition.

2.5.11. Field Exposure

Considering the importance of evaluating also the durability of stone consolidants [38] and that small differences in microclimatic conditions may have a strong impact on stone durability [58], untreated and treated stone specimens were exposed in the cave for 9 months (from April to December 2019) to obtain a preliminary evaluation of the effects of the specific environmental conditions inside the Magura cave (T = 12–25 °C, RH = 65–90%). The exposed samples were periodically monitored by visual observation.

3. Results and Discussion

3.1. Morphology of the New Phases

The morphology of the new phases formed after treatment is illustrated in Figure 4.

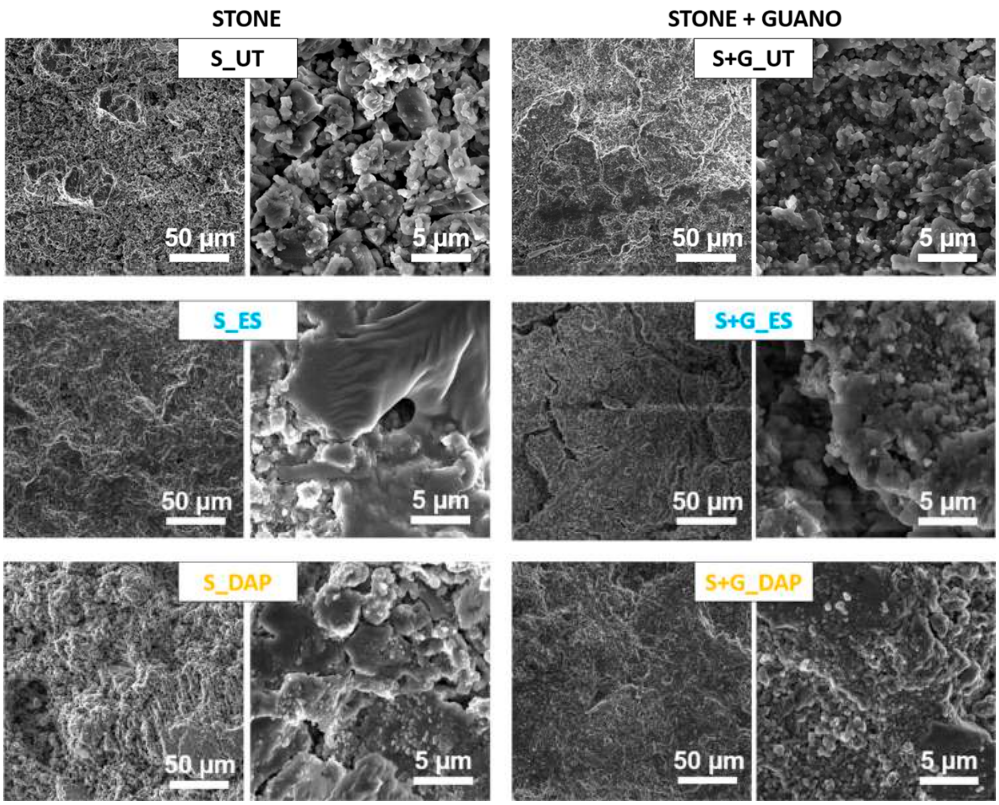

Figure 4. Morphology of untreated and treated stone ("ST") and stone+guano (ST+G") specimens.

In the case of the "ST" specimens, the untreated stone was characterized by large pores among the calcite crystals. After consolidation with "ES", a coating of amorphous silica was formed, as expected [41]. Because of the porous nature of the substrate, the coating was not continuous, and bare areas were largely visible. After treatment with "DAP", small clusters of the new calcium phosphates were visible on the stone surface, which, also in this case, was not continuously coated with the new phases. Generally, new calcium phosphates formed in carbonate stones from the reaction with ammonium phosphate solutions show a flower-like morphology [25], but, in the case of dilute solutions (such as that adopted in the present case), the formation of small clusters has been reported before [59,60].

In the case of the "ST+G" specimens, observation of the untreated sample at low magnification allowed to distinguish the scales constituting the guano layer, which was cracked and prone to detachment from the substrate. After consolidation with "ES", cracks were still visible in the guano layer. The tendency of the silica gel formed from ethyl silicate to crack upon drying is well known [41]. An increase in the cohesion of the guano layer seemed to be present in the case of the "DAP" specimen, where tiny crystals, ascribable to the formation of the new calcium phosphates, were visible over the treated surface.

3.2. Composition of the New Phases

The FT-IR spectra of untreated and treated specimens are reported in Figure 5.

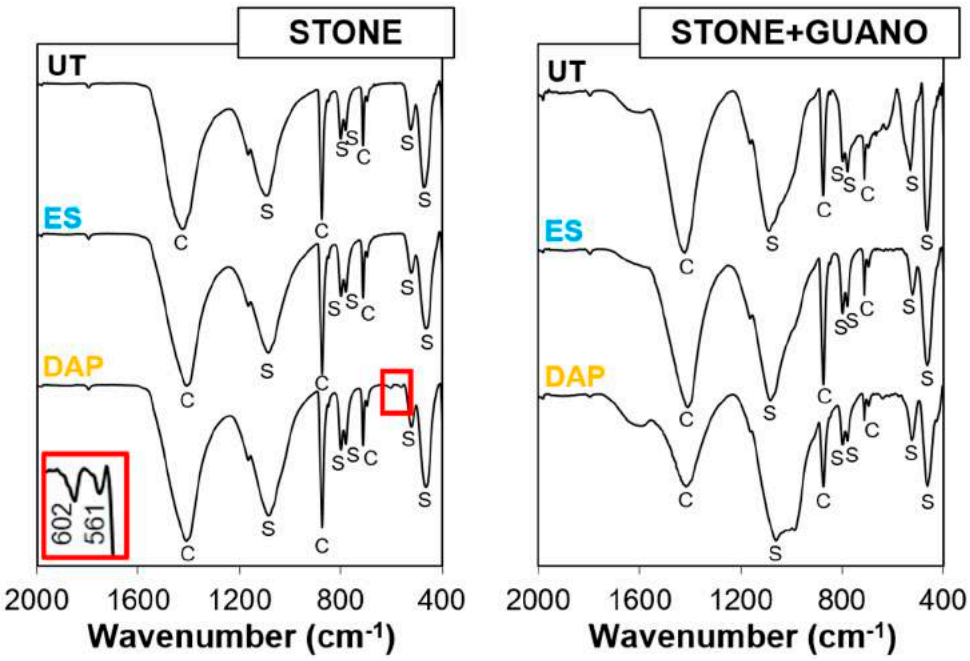

Figure 5. FT-IR spectra of untreated and treated stone ("ST") and stone+guano (ST+G") specimens. C = Calcite; S = Silica; new bands at 602 and 561 cm^{-1}, owing to the formation of new calcium phosphate phases, are highlighted in the inset.

In the "ST" specimens, bands owing calcite and silica were present in the untreated reference. After treatment with "ES", no new band was visible because "ES" led to the formation of amorphous silica, whose bands overlapped with those of the substrate. After treatment with "DAP", small new bands appeared at 602 and 561 cm^{-1}, which indicated the formation of new calcium phosphates [61]. The fact that these new bands were very small was due to the low concentration of DAP used for the treatment (0.1 M), which was consistent with a previous study where FT-IR bands of new calcium phosphates were found to be more pronounced for more concentrated DAP solutions [60]. To distinguish between formation of hydroxyapatite [HAP, $Ca_{10}(PO_4)_6(OH)_2$] and octacalcium phosphate

[OCP, $Ca_8H_2(PO_4)6{\cdot}5H_2O$], which both could be formed as the reaction product between calcareous stones and DAP solutions [51] and both have FT-IR bands at 560–563 and 600–602 cm^{-1} [61], the position of the other strong bands (at 1031 cm^{-1} for HAP and 1023 cm^{-1} for OCP [61]) should be considered. However, in the present case, no other band was clearly visible because of the overlapping with the strong band at 1080 cm^{-1} owing to quartz in the substrate. Consequently, no conclusive identification of the new phase was possible. However, the formation of either hydroxyapatite or octacalcium phosphate was expected to have a durable consolidating ability, as both minerals have lower water solubility than calcite [25,51].

In the case of the "ST+G" specimens, the spectrum of the untreated reference exhibited some new shoulders at 1580, 1000, and 700 cm^{-1} (not present in the untreated "ST" sample), which could be attributed to the guano layer. These shoulders were present also in the FT-IR spectra of the treated "ST+G" samples, which exhibited no additional clear band owing to new phase formation. In the case of "ES", this was not surprising, for the reasons discussed above. In the case of "DAP", the lack of new bands (contrary to the case of the "ST" sample) was most likely due to the very low amount of new phases formed after treatment. In fact, very little amounts of new phases are usually formed [22], especially when diluted DAP solutions are used [25]. Moreover, in the present case, the guano layer likely acted as a barrier, limiting the consolidant penetration (cf. Section 3.3) and reducing the number of new phases. Although below the detection limit of FT-IR, new phases were, however, formed after treatment, as indicated by the significant mechanical improvement (cf. Sections 3.4 and 3.5).

3.3. Penetration Depth

The penetration depth of the "ES" and "DAP" treatments into the "ST" and "ST+G" samples, measured by fracturing the samples right at the end of the consolidant application, is illustrated in Figure 6.

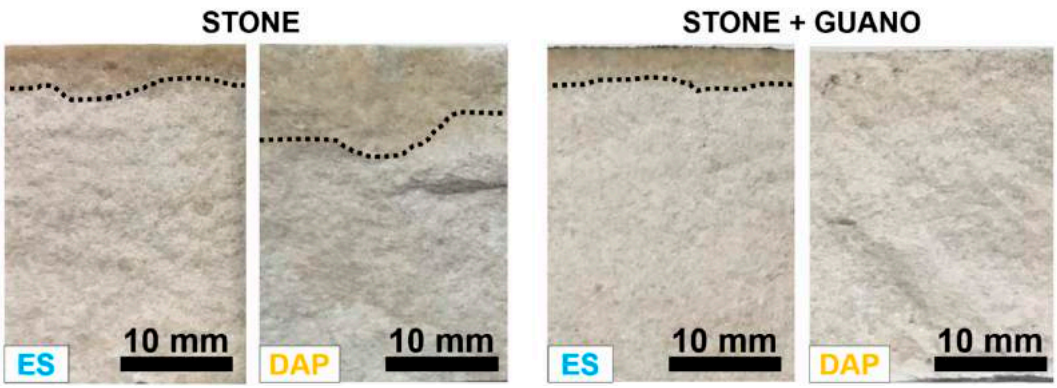

Figure 6. Examples of penetration depth of the treatments into the stone and stone+guano samples.

In the case of the stone specimens, the penetration depth was 4.5 ± 1 mm for "ES" and 7.0 ± 1.0 mm for "DAP", the limit of the wet fringe being more easily distinguishable in "ES" specimens. Such penetration depth of both consolidants was in line with previous results if the porosity of the substrate was considered: a penetration >10 mm was reported for both ES [42] and DAP [26,42,62] for highly porous limestones (open porosity 35–50%), while values between 3 and 5 mm were reported for less porous stones (open porosity 5–17%) [30,40]. It is worth noting that previous studies highlighted that, during curing, consolidants are progressively absorbed into finer pores [12], so that the final depth of formation of new binding phases is generally higher than assessed right at the end of the consolidant application [38,63].

In the case of the "ST+G" specimens, the penetration depth was 3.5 ± 1 mm for "ES", hence slightly lower compared to the "ST" specimens. This reduction in penetration depth was likely due to the guano layer acting as a barrier and altering the penetration into the substrate. Moreover, because

the consolidants were applied 30 min after application of the guano layer, some water used to apply the guano might have been still present in the pores of the samples, thus reducing the ability of the consolidants to penetrate in depth. In the case of "DAP", no evident sign of a wet fringe could be observed. Nonetheless, this was not an indication that no penetration took place because, otherwise, there would be no mechanical improvement, contrary to what assessed in Sections 3.4 and 3.5.

3.4. Dynamic Elastic Modulus

For untreated and treated "ST" and "ST+G" specimens, E_d values measured in the directions perpendicular and parallel to the plane of the slabs are reported in Figure 7.

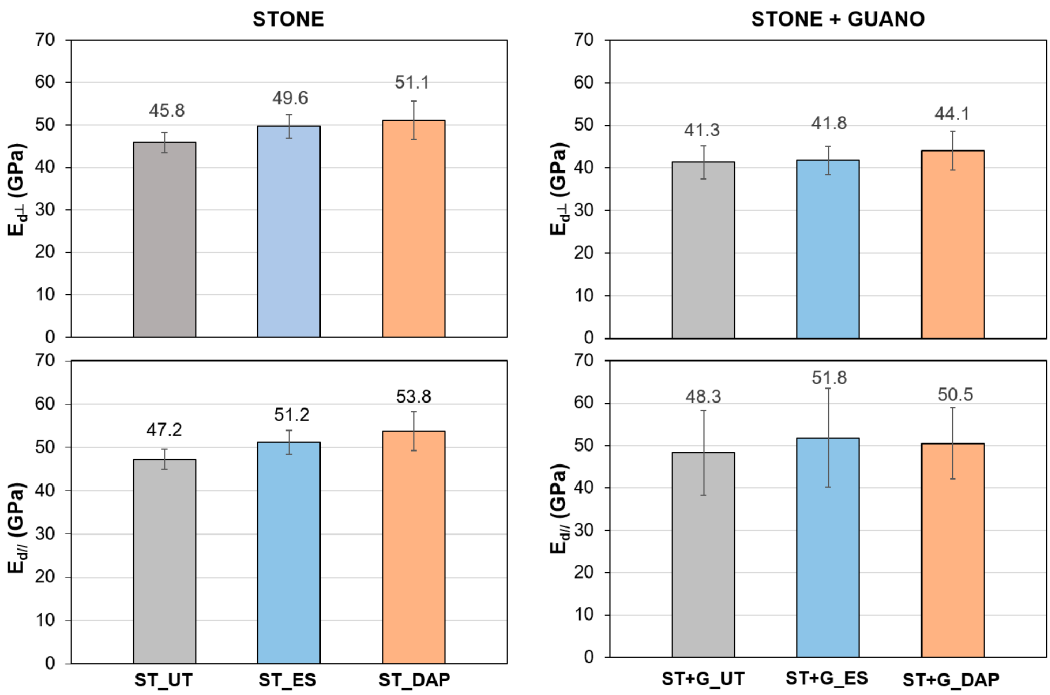

Figure 7. Dynamic elastic modulus (E_d) of untreated ("UT") and treated ("ES" and "DAP") stone ("ST") and stone+guano ("ST+G") specimens in the directions perpendicular and parallel to the plane of the slab.

In the "ST" specimens, both treatments caused an improvement in E_d, the increase being higher in the case of the "DAP" treatment. Indeed, the "ES" treatment caused an E_d increase of +8% in the perpendicular direction and +8% in the parallel direction, whereas the "DAP" treatment caused an E_d increase of +11% in the perpendicular direction and +14% in the parallel direction. The fact that the DAP treatment resulted more effective than ES was in line with several previous studies on limestone consolidation by these two consolidants: the increase in E_d was +15% for DAP and +11% for ES in Pietra Serena [28], +9–11% for DAP and +7% for ES in Arenisca Ronda [39], +90–110% for DAP and +42% for ES in Indiana limestone [22,48]. In other comparative studies, ES caused higher E_d increases than DAP: +25% for DAP and +39% for ES in Giallo di Siena [28] and +47% for DAP and +62% for ES in Globigerina limestone [42]. In any case, when comparing results obtained in different studies, it should be borne in mind that the properties of the stones tested in each study (mineralogical composition, open porosity, and pore size distribution) and the properties of the tested consolidants (concentration of the active principle, nature and amount of the solvent, application technique, etc.) play a fundamental role, determining the final outcome of the consolidating treatment.

As for the "ST+G" specimens, in the untreated condition, they exhibited a lower E_d value in the perpendicular direction compared to the "ST" specimens (41.3 ± 3.9 GPa against 45.8 ± 2.3 GPa, respectively), while, in the parallel direction, the values were much closer (48.3 ± 10.1 GPa against

47.2 ± 3.8 GPa, respectively). This was thought to be a consequence of the guano presence in the "ST+G" specimens, where the guano layer worsened the contact between the specimen and the transducers in the perpendicular direction, while no alteration was present in the parallel direction. The guano presence also slightly reduced the consolidating effectiveness. In fact, the "ES" treatment caused an E_d increase of +1% in the perpendicular direction and +7% in the parallel direction, while the "DAP" treatment caused an E_d increase of +7% in the perpendicular direction and +4% in the parallel direction. This reduction, compared to the "ST" samples, was most likely due to the guano layer, limiting the consolidant penetration in depth and thus the consolidating ability in the "ST+G" specimens.

3.5. Resistance to Abrasion

The weight losses of untreated and treated specimens after the abrasion test are reported in Figure 8.

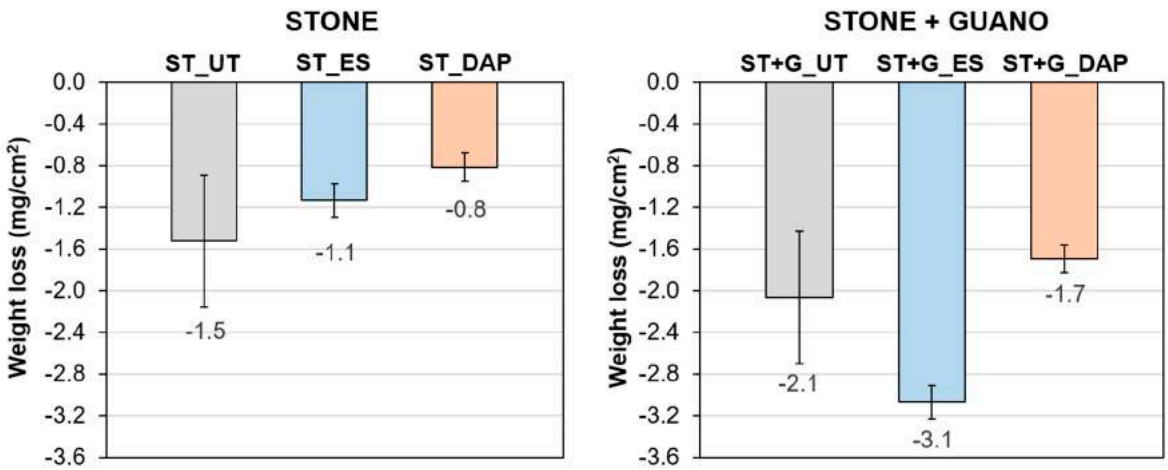

Figure 8. Weight loss after the abrasion test of untreated ("UT") and treated ("ES" and "DAP") stone ("ST") and stone+guano ("ST+G") specimens.

In the case of the "ST" specimens, both consolidants improved the stone resistance to abrasion, again the benefit being higher for the "DAP" treatment, consistent with the E_d results. Indeed, the "ES" treatment caused a reduction in weight loss by 26%, whereas the "DAP" treatment caused a reduction by 47%. The higher efficacy of DAP to increase stone resistance to abrasion was consistent with previous results obtained on marble (reduction in the weight loss by 86% for DAP and 60% for ES [64]), while substantially similar results were obtained for the two treatments on highly porous limestone (reduction in the weight loss by 37% for both DAP and ES [42]).

In the case of the "ST+G" specimens, the untreated references exhibited a higher weight loss compared to the "ST" specimen because the guano layer could be easily detached from the stone substrate. In the case of the treated specimens, as already noticed in the case of E_d, the guano layer interfered with the consolidant penetration and hardening, so that a lower benefit was found, compared to the "ST" specimens. In particular, the "DAP" treatment caused an improvement in the resistance to abrasion (weight loss reduced by 18%), while the "ES" treatment apparently worsened the resistance to abrasion. In fact, compared to the untreated condition, the "ES" treatment apparently caused an increase in weight loss by 49%. This was thought to occur because the "ES" treatment deposits a relatively high amount of new material in the porous guano layer so that the removal of the guano layer during the abrasion test results in a high weight loss.

3.6. Color Change

The appearance of an illustrative specimen for each condition of the "ST" and "ST+G" specimens is shown in Figure 9. The measured CIELab color parameters are reported in Table 1.

In the case of the "ST" specimens, the "ES" treatment caused some darkening (decrease in L^*) and shift towards red (increase in a^*). The general tendency of ethyl silicate to darken the treated stone is well known [39,41,42]. On the contrary, the "DAP" treatment caused some whitening (increase in L^*) and shift towards blue (decrease of b^*), as also assessed in previous studies [26,40,64,65]. For both treatments, the resulting color change was lower than the threshold commonly accepted for conservation treatments ($\Delta E^* = 5$ [66]), as illustrated in Figure 10. In the case of the "DAP" treatment, a color change lower than the acceptability threshold is usually experienced [25], even though more pronounced color changes have been reported in the literature [39]. However, for a given consolidant, the color change strongly depends on a multiplicity of parameters, such as the initial color of the stone, the consolidant concentration, and the application technique [39].

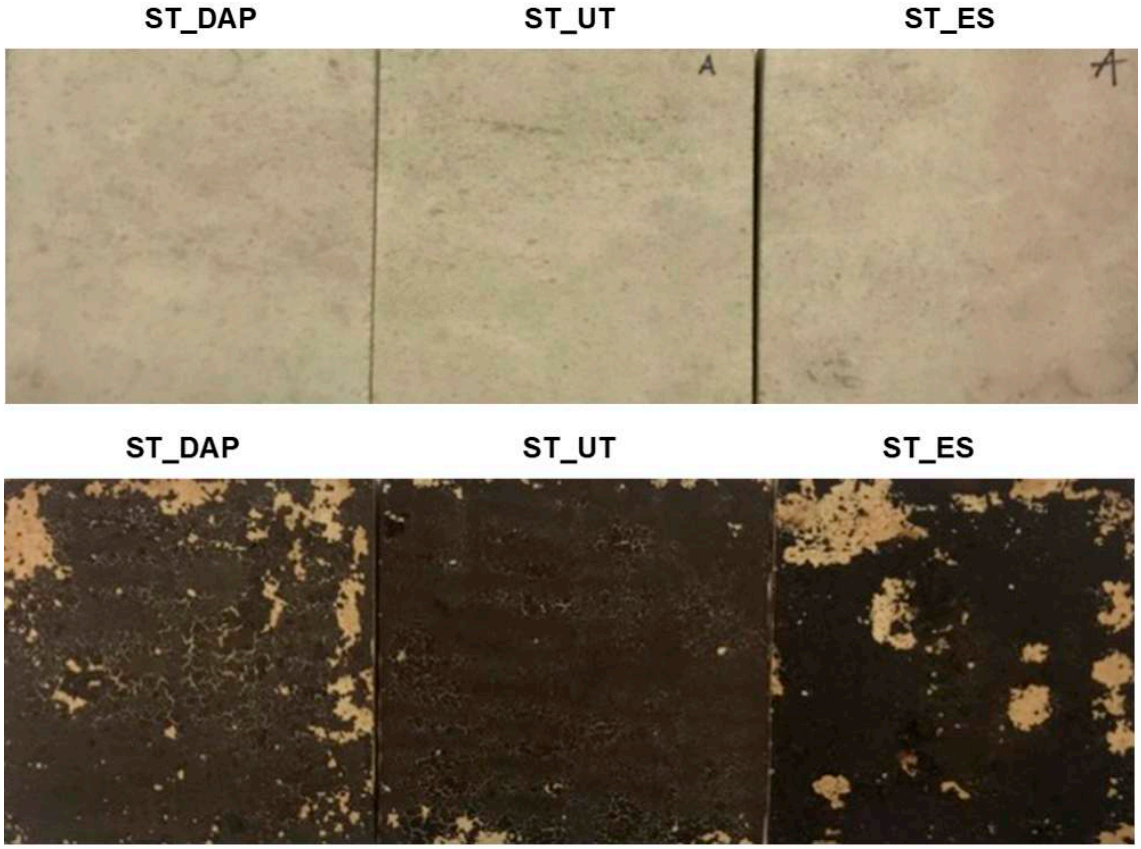

Figure 9. Comparison between the surface appearance of "DAP"-treated (**left**), "UT" (**middle**), and "ES"-treated (**right**) stone ("ST") and stone+guano ("ST+G") specimens. DAP = diammonium hydrogen phosphate; UT = untreated; ES = ethyl silicate.

Table 1. Color parameters of untreated and treated specimens.

Specimens	Condition	L^*	a^*	b^*
ST	UT	79.55 ± 0.76	2.86 ± 0.18	10.36 ± 0.58
	ES	77.20 ± 2.16	4.07 ± 0.90	10.90 ± 1.90
	DAP	81.10 ± 1.22	2.53 ± 0.23	8.98 ± 0.28
ST+G	UT	29.13 ± 1.17	6.31 ± 0.85	7.02 ± 0.29
	ES	24.91 ± 0.88	6.46 ± 1.20	4.70 ± 0.43
	DAP	32.25 ± 1.39	5.29 ± 0.55	7.24 ± 0.31

"ST" = stone, "ST+G" = stone+guano, "UT" = untreated, "ES" = ethyl silicate, "DAP" = diammonium hydrogen phosphate, L^* = black–white, a^* = green–red, b^* = blue–yellow.

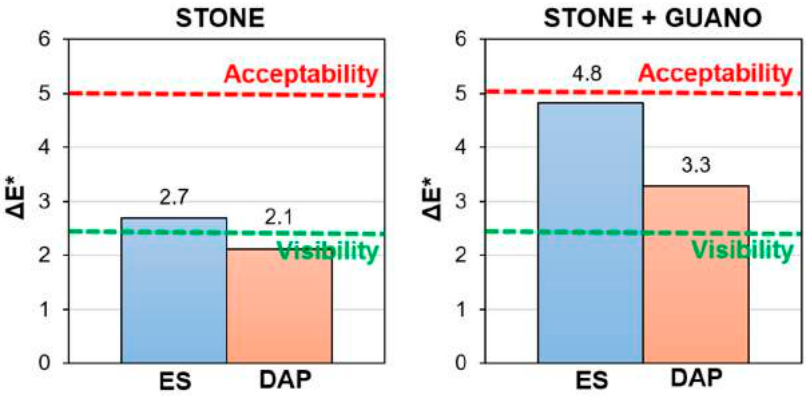

Figure 10. Color change (Δ*E**) of stone ("ST") and stone+guano ("ST+G") specimens.

In the case of the "ST+G" specimens, the color alteration after consolidation was higher than in the "ST" specimens, again because the guano layer partly interfered with the consolidant penetration into the substrate. This resulted in a considerable darkening in the case of the "ES" treatment (significant decrease in *L**) and considerable whitening in the case of "DAP" (significant increase in *L**). As reported in Figure 10, the resulting color change Δ*E** was anyway lower than the common acceptability threshold (Δ*E** = 5 [66]). However, in this specific case, a general visual assessment of the alteration of the surface appearance (Figure 9) was probably more significant to evaluate the impact of the treatments because both consolidants (especially "DAP") caused some increase in the cracking of the guano layer, thus making the color measurement difficult. This increase in cracking was likely the result of combined mechanical stress originated by the brush stroke and physical stress originated by the solvents in which the consolidants were dissolved (water and ethanol in the case of DAP, isopropyl alcohol in the case of ES).

3.7. Pore Size Distribution

The pore size distribution of a representative sample for each condition is illustrated in Figure 11. In the "ST" specimens, the "DAP" treatment caused minor alterations in pore size distribution and total open porosity, which decreased from 17.9% to 14.2%. A limited reduction in open porosity after the DAP treatment was consistent with previous results on limestone consolidation by several formulations of the treatment [22,28,40,42]. The "ES" treatment caused a more pronounced reduction in open porosity (from 17.9% to 10.7%), which again was in line with the tendency reported in the literature [41,42,47]. Such different impact of the two consolidants on the pore system of the treated stone was in line with previous findings, and it was one of the major differences between the two consolidating treatments [28,42].

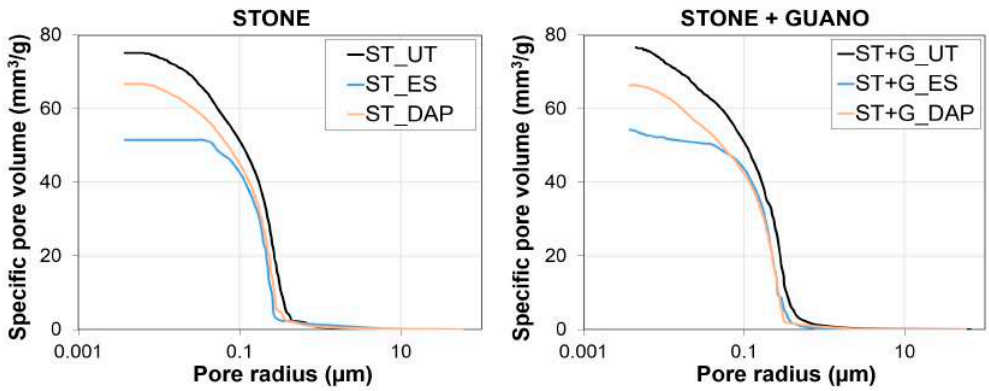

Figure 11. Pore size distributions of untreated ("UT") and treated ("ES" and "DAP") specimens of stone ("ST") and stone+guano ("ST+G").

Substantially similar behavior was registered also in the case of the "ST+G" specimens, where the presence of the guano layer apparently had very little effect on the MIP measurement, even in the untreated sample. This was a consequence of the fact that, during the MIP test, mercury can be intruded into the sample not only through the sample face covered with the guano layer but also through the other faces of the sample (free from guano), so that the influence of the guano layer is strongly reduced.

3.8. Static Contact Angle

The values of static contact angle measured for the "ST" specimens in the various conditions are summarized in Figure 12, which also displays examples of static contact angle photographed for "ST" and "ST+G" specimens.

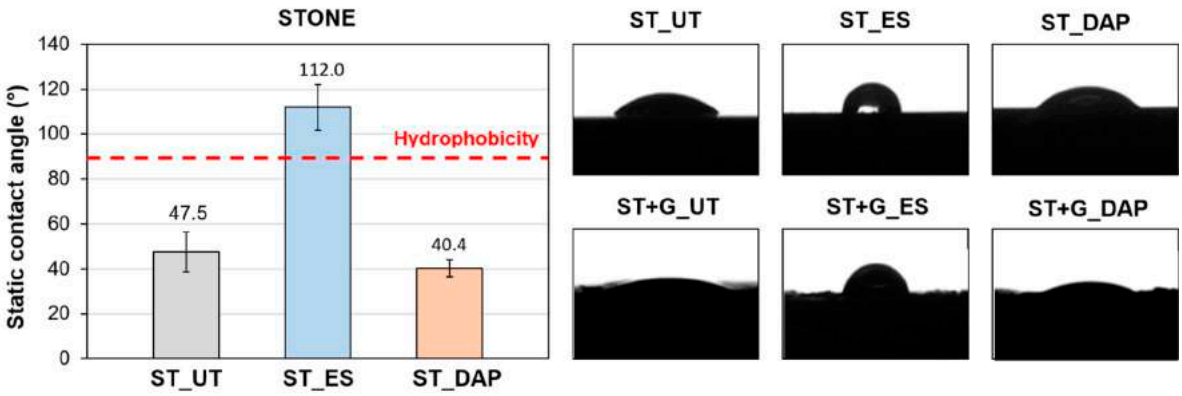

Figure 12. Values of static contact angle of untreated ("UT") and treated ("ES" and "DAP") stone specimens ("ST") and photos of the static contact angle of both "ST" and "ST+G" specimens.

The untreated "ST" sample exhibited a hydrophilic behavior, as expected (contact angle 47.5° ± 8.9°). The "DAP" treatment caused a slight alteration in the contact angle, which slightly diminished to 40.4° ± 3.9°. Such reduced alteration in stone wettability was consistent with previous results [42]. On the contrary, the "ES" treatment caused a sensible increase in the contact angle up to 112.0° ± 10.2°, so that, 8 weeks after treatment, the stone was still hydrophobic. As discussed in Section 1, products based on ethyl silicate are known to cause prolonged hydrophobicity, lasting up to 6–7 months [12,41,47]. Nonetheless, it is worthy to highlight that the technical data sheet of the commercial product used in this study states that the product reaction is complete in about 4 weeks, while curing is evidently still in progress after 8 weeks.

In the case of the "ST+G" specimens, it was impossible to quantify the static contact angle with the adopted software because the roughness of the guano layer was too high for the software to identify a straight baseline for the contact angle calculation. However, from a qualitative point of view, the same behavior observed for the "ST" samples was confirmed also for the "ST+G" samples, as illustrated in Figure 12. The "ES"-treated stone exhibited a clear hydrophobic behavior, whereas the "DAP"-treated one remained hydrophilic.

3.9. Water Sorptivity and Water Absorption

For untreated and treated specimens, the weight increase per unit area as a function of time is illustrated in Figure 13, while the resulting water sorptivity (S), water absorption after 24 h (WA_{24h}), and water absorption after 7 days (WA_{7d}) are reported in Table 2.

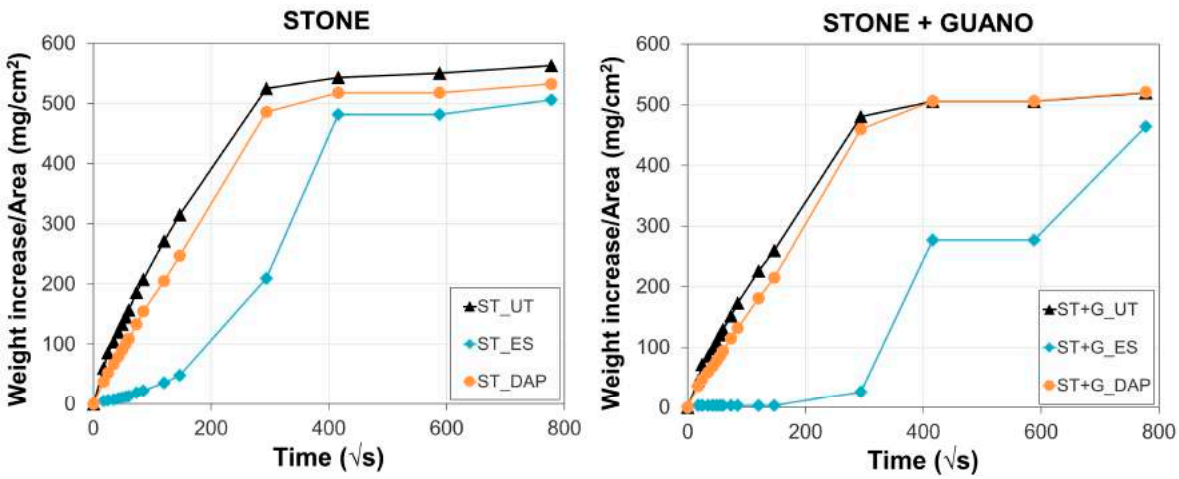

Figure 13. Water absorption as a function of time of untreated ("UT") and treated ("ES" and "DAP") stone ("ST") and stone+guano ("ST+G") specimens.

Table 2. Water transport properties of untreated and treated specimens.

Specimens	Condition	S (mg/cm^2 √s)	WA_{24h} (wt.%)	WA_{7d} (wt.%)
ST	UT	1.79 ± 0.14	4.9 ± 0.4	5.2 ± 0.4
	ES	n.d.	1.9 ± 0.8	4.6 ± 0.1
	DAP	1.65 ± 0.06	4.5 ± 0.2	4.9 ± 0.3
ST+G	UT	1.64 ± 0.01	4.0 ± 0	4.7 ± 0
	ES	n.d.	0.2 ± 0	4.1 ± 0.1
	DAP	1.57 ± 0.05	4.2 ± 0.1	4.8 ± 0

"ST" = stone, "ST+G" = stone+guano, "UT" = untreated, "ES" = ethyl silicate, "DAP" = diammonium hydrogen phosphate, *S* = water sorptivity, WA_{24h} = water absorption after 24 h, WA_{7d} = water absorption after 7 days, n.d. = not determinable (because of the initial hydrophobic behavior).

Consistently with the slight alterations in static contact angle and pore size distribution, the "DAP" treatment caused only minor modifications in stone sorption properties, leading to minor changes in the final water absorption after 24 h (4.5 ± 0.2 wt.% for "DAP" against 4.9 ± 0.4 for "UT") and after 7 days (4.9 ± 0.3 wt.% for "DAP" against 5.2 ± 0.4 for "UT"). This was consistent with the previous results obtained on several types of stone treated by DAP [25,28,39,42].

On the contrary, the water absorption of "ES"-treated samples was initially very low, reaching a water absorption of 1.9 ± 0.8 wt.% after 24 h. After prolonged contact with water, the hydrophilic behavior of the stone was re-established, so that water absorption after 7 days was close to that of the untreated stone (4.6 ± 0.1 wt.% for "ES", 5.2 ± 0.4 for "UT"). The period during which stone remains hydrophobic (which in the field can last up to 6–7 months [47]) may threaten stone durability. Indeed, if water containing dissolved salts is trapped behind the consolidated layer, salt crystallization behind the consolidated layer may lead to detachment of this layer, thus causing failure of the conservation work [12]. For this reason, conservation treatments that do not significantly alter stone transport properties are often preferred [38].

In the case of the "ST+G" samples, the water sorptivity and the amount of water absorbed after 24 h and 7 days were a little lower, compared to the "ST" samples, likely because of the presence of the guano layer. Nonetheless, similar to the previous case, the "DAP" treatment basically caused no modification in the absorption capacity, while the "ES" treatment induced an initial hydrophobic behavior.

Because of their initial hydrophobic behavior, the sorptivity value S of the "ES"-treated specimens could not be determined.

3.10. Water Vapor Permeability

The water vapor diffusion resistance coefficient (μ) of untreated and treated "ST" specimens is reported in Table 3. The "DAP" treatment left the μ coefficient substantially unaltered, which was consistent with the modest reductions measured in previous studies on stone consolidation by DAP [40,42]. The "ES" treatment was found to cause a significant reduction in the water vapor permeability, differently from a previous study on a more porous limestone where a negligible reduction was found after treatment with ethyl silicate [42]. It is true that, also, in the present case, the vapor exchange with the environment was not completely blocked, but still a considerable reduction in water vapor permeability might be an issue for the conservation of the Magura cave paintings; hence, this aspect requires further investigation.

In the case of the "ST+G" specimens, the adopted method to test the water vapor permeability resulted as unsuitable. In fact, because the face of the specimens covered with the guano layer and treated with the consolidant was placed downwards (to ensure that the water vapor cross the consolidated layer), during the test, flakes of guano started to detach and fell into the KNO_3 solution, thus altering the reliability of the test results. For this reason, no μ values were available in the case of the "ST+G" specimens, although a behavior substantially similar to that exhibited by the "ST" specimens was expected.

Table 3. Water vapor diffusion resistance coefficient of untreated and treated stone specimens.

Specimens	Condition	μ
ST	UT	47.8 ± 0.7
	ES	82.4 ± 11.6
	DAP	45.8 ± 0.9

"ST" = stone, μ = water vapor diffusion resistance coefficient (absolute number).

3.11. Field Exposure

After exposure in the cave from April to December 2019, none of the specimens exhibited visible alteration, such as biodeterioration or pulverization. Of course, field exposure for 9 months was not enough to derive conclusive information on the long term behavior of the treated stone. Nonetheless, considering the very specific environmental conditions in the cave, this period of time was likely sufficient to trigger weathering processes, such as salt crystallization and growth of microorganisms, so the lack of visible deterioration after 9 months could be regarded as an encouraging result.

3.12. Pre-treatment by Plasma

For untreated stone specimens, the alteration in static contact angle measured 30 min after the plasma treatment (corresponding to the time between plasma pre-treatment and consolidant application) is qualitatively illustrated in Figure 14. The plasma treatment definitely modified the wettability of the stone, substantially increasing its hydrophilicity.

Nonetheless, the increase in wettability did not significantly alter the penetration depth of the consolidants, as indicated by results of consolidant uptake and mechanical strengthening reported in the following. The weight gain at the end of the consolidant application was substantially the same for specimens pre-treated or not by plasma, as illustrated in Figure 14. This was thought to be a consequence of the fact that the plasma treatment significantly modifies the wettability of the stone surface, but the walls of the pores inside the stone maintain the original properties so that the mechanism of liquid absorption in depth and the resulting penetration depth and liquid uptake are not significantly modified. Consistently, no improvement in the consolidating ability was evidenced in the case of samples pre-treated by plasma before consolidant application, as indicated by dynamic elastic modulus measurements (Figure 14).

From these results, pre-treatment by plasma looks like a promising strategy for the application of conservation treatments that are intended to affect mostly the stone surface (such as protective treatments). In the case of conservation treatments aimed at penetrating in depth into the stone (such as consolidating treatments), no clear benefit seems to derive from pre-treatment by plasma because the wettability of the stone surface is modified but, inside the pores, the wettability of the pore walls remains substantially unaltered.

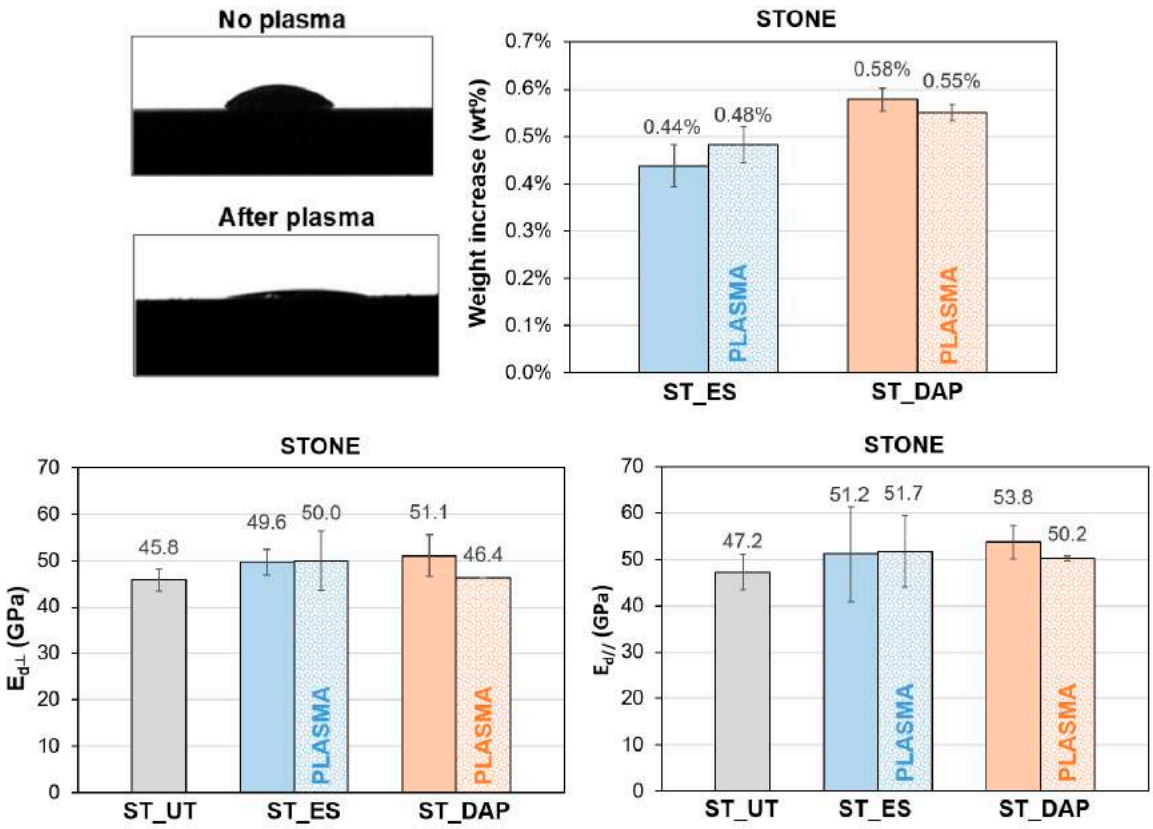

Figure 14. Effects of pre-treatment by plasma on the static contact angle of untreated stone ("ST_UT") specimens, weight increase of the stone specimens ("ST") at the end of the treatment application, and dynamic elastic modulus (E_d) of untreated ("UT") and treated ("ES" and "DAP") stone specimens ("ST"), without (solid bars) and with (dotted bars) pre-treatment by plasma, in the directions perpendicular and parallel to the plane of the slab.

4. Conclusions

Based on the results obtained in the present study, aimed at evaluating the effectiveness and the compatibility of two alternative consolidants taken into consideration for the conservation of prehistoric paintings in the Magura cave (Bulgaria), the following conclusions could be derived:

- In the case of the stone specimens, both the treatment based on ethyl silicate ("ES") and that based on ammonium phosphate ("DAP") were able to increase stone mechanical properties, the increase being higher for "DAP". Both treatments caused acceptable color changes, while a significant difference was registered in terms of alterations in water and water vapor transport properties. "DAP" left the stone hydrophilic, with negligible alterations in static contact angle and water sorptivity, while "ES" made the stone hydrophobic, even 8 weeks after the consolidant application. Moreover, "DAP" also left the water vapor permeability basically unaltered, while a reduction in permeability was caused by "ES". After exposure in the cave for 9 months, none of the treated specimens had shown evident signs of biodeterioration or pulverization, which could be regarded

as an encouraging result, even though long term data are necessary to conclusively ascertain the treatment durability.

- In the case of the stone+guano specimens, the presence of the guano layer affected the penetration of the two consolidants into the stone, thus partly reducing the consolidating effectiveness. A more intense color change was registered, compared to the stone samples, alongside cracking of the guano layer. Although more difficult to quantify, the general trend of modification in water transport properties was confirmed: "DAP" caused minor alterations, while "ES" made the stone+guano specimens hydrophobic. It was not possible to reliably determine the water vapor permeability of the stone+guano specimens by the adopted methodology, but results substantially similar to those of the stone specimens were expected (similarly to the case of the water transport properties).
- Regarding the possible benefit deriving from pre-treatment by non-thermal plasma before consolidant application, a significant decrease in the static contact angle of the stone surface was found after plasma treatment. This might be useful for the application of conservation treatments that are intended to remain mostly on the stone surface (e.g., protective treatments). Nonetheless, no significant increase in the amount of retained product or mechanical consolidation was found when pre-treatment by plasma was performed because the wettability of the stone surface was conveniently modified, but that of the pore walls remained unaltered.

All things considered, the comparison between the two investigated consolidants suggested that the "DAP" treatment had the advantage of causing higher mechanical strengthening, with lower alterations in stone transport properties, compared to the "ES" treatment. This latter aspect is very important, especially in the case of the Magura cave, where rising damp containing dissolved salts might trigger severe conservation issues if it was blocked behind a hydrophobic layer, which might be the case of the "ES" treatment. Moreover, in the case of a moist substrate (as likely the case inside the cave), the "DAP" treatment had the advantage of being applicable even if the stone pores were partly filled with water. On the contrary, the application of ES-based products would be impossible, as they react readily with water, so that deep penetration and bonding of the stone grains would be prevented.

However, the present study was based on several simplifications, which made the effects of the two treatments easier to be evaluated, but still not fully representative of the real conditions in the cave. In particular, the following aspects need to be further evaluated in future research, before any consolidant is applied onto the real artworks:

- the presence of the surface guano layer: an improved methodology of guano application onto the limestone substrate needs to be developed. In fact, the methodology adopted in this study produced specimens very prone to pulverization and detachment of the guano layer, differently from the real guano paintings in the Magura cave. To reproduce the paintings in a manner that fully resembles the condition of the real ones is extremely difficult, as the prehistoric paintings have undergone millennials of fossilization. A possible strategy to improve the reliability of the stone+guano specimens produced in the laboratory may be to subject the stone+guano specimens to accelerated aging, aimed at mimicking the natural fossilization process.
- the presence of salts in the substrate: after evaluating the effects of the two consolidants onto uncontaminated specimens, their effects onto specimens containing salts in the pores need to be evaluated, as this would be the condition in the cave (complete salts removal before the consolidant application is not feasible). To do so, the amount and nature of the salts present in the limestone cave need to be specifically investigated and characterized, so that laboratory specimens can be prepared accordingly. Then, after preliminary salt contamination and consolidation, the durability of the treated specimens to further salt weathering should be evaluated by accelerated salt crystallization cycles. This should be carried out in the current environmental conditions of the cave or, in case it is possible to control them, in the adjusted environmental conditions that would be adopted for cave conservation.

In conclusion, the present study does not complete the research needed to address the complex issue of preserving the prehistoric paintings in the Magura cave but represents the first step towards this goal.

Author Contributions: Conceptualization, M.S., Z.K., E.S., and E.F.; methodology, E.S., E.F., P.S., and E.V.F.; investigation, E.S., E.F., P.S., and E.V.F.; visualization, E.S.; writing—original draft preparation, E.S.; writing—review and editing, E.F., M.S., Z.K., P.S., and E.V.F. All authors have read and agree to the published version of the manuscript.

Funding: This research received no external funding.

Acknowledgments: Marta Ripà is gratefully acknowledged for collaboration to the experimental tests.

Conflicts of Interest: The authors declare no conflict of interest.

References

1. Ivanova, S.; Gurova, M.; Spassov, N.; Hristova, L.; Tzankov, N.; Popov, V.; Marinova, E.; Makedonska, J.; Smith, V.; Ottoni, C.; et al. Magura Cave, Bulgaria: A multidisciplinary study of Late Pleistocene human palaeoenvironment in the Balkans. *Quatern Int.* **2016**, *415*, 86–108. [CrossRef]
2. Stoytchev, T. Eneolithic paintings from Magoura cave, Bulgaria. *Annu. Dep. Archaeol. NBU* **1994**, *1*, 307–320. (In Bulgarian)
3. Stoytchev, T. *Rock Art: General Classification*; Agato Press: Sofia, Bulgaria, 2005; p. 24. (In Bulgarian)
4. Nougier, R. Les "ballerines" de Magura. *Préhistoire Ariégeoise* **1977**, *XXXII*, 123–131.
5. Kunov, A.; Arnaudov, V.; Molar, M. First ^{14}C dating of the bat guano used for the ancient drawings of Magura cave, NW Bulgaria. In Proceedings of the Bulgarian Geological Society, National Conference "GEOSCIENCES 2014", Sofia, Bulgaria, 10–11 December 2014.
6. *Illustrated Glossary on Stone Deterioration Patterns = Glossaire Illustré sur les Forms D'altération de la Pierre*, 1st ed.; Vergès-Belmin, V. (Ed.) English-French ed.; Monuments & Sites no. 15; ICOMOS and (ISCS) International Scientific Committee for Stone: Paris, France, 2008.
7. Mitova, M.M.; Iliev, M.; Nováková, A.; Gorbushina, A.A.; Groudeva, V.I.; Martin-Sanchez, P.M. Diversity and biocide susceptibility of fungal assemblages dwelling in the Art Gallery of Magura Cave. *Bulg. Int. J. Speleol.* **2017**, *46*, 67–80. [CrossRef]
8. Stefanova, M.; Kamenarov, Z.; Sassoni, E.; Franzoni, E.; Ripà, M.; Patelli, A.; Scopece, P.; Verga Falzacappa, E.; Sakaj, M. Innovative solutions for prehistoric paintings -atmospheric pressure plasma and phosphate consolidant for the preservation of the Magura Cave (Bulgaria) 13–15 May 2020. *Florence (IT) Proc. Heri-Tech* **2020**, in press.
9. Chelazzi, D.; Poggi, P.; Jaidar, Y.; Toccafondi, N.; Giorgi, R.; Baglioni, P. Hydroxide nanoparticles for cultural heritage: Consolidation and protection of wall paintings and carbonate materials. *J. Colloid Interface Sci.* **2013**, *392*, 42–49. [CrossRef]
10. Valladas, H.; Cachier, H.; Maurice, P.; Bernaldo de Quirost, F.; Clottes, J.; Cabrera Valdes, V.; Uzquiano, P.; Arnold, M. Direct radiocarbon dates for prehistoric paintings at the Altamira, EI Castillo and Niaux caves. *Nature* **1992**, *357*, 68–70. [CrossRef]
11. Chalmin, E.; Vignaud, C.; Menu, M. Palaeolithic painting matter: Natural or heat-treated pigment? *Appl. Phys. A* **2004**, *79*, 187–191. [CrossRef]
12. Scherer, G.W.; Wheeler, G.S. Silicate consolidants for stone. *Key Eng. Mater.* **2009**, *391*, 1–25. [CrossRef]
13. Baglioni, P.; Carretti, E.; Chelazzi, D. Nanomaterials in art conservation. *Nat. Nanotechnol.* **2015**, *10*, 287–290. [CrossRef]
14. Rodriguez-Navarro, C.; Ruiz-Agudo, E. Nanolimes: From synthesis to application. *Pure Appl. Chem.* **2018**, *90*, 523–550. [CrossRef]
15. Ambrosi, M.; Dei, L.; Giorgi, R.; Neto, C.; Baglioni, P. Colloidal Particles of $Ca(OH)_2$: Properties and Applications to Restoration of Frescoes. *Langmuir* **2001**, *17*, 4251–4255. [CrossRef]
16. Giorgi, R.; Ambrosi, M.; Toccafondi, T.; Baglioni, P. Nanoparticles for Cultural Heritage Conservation: Calcium and Barium Hydroxide Nanoparticles for Wall Painting Consolidation. *Chem. Eur. J.* **2010**, *16*, 9374–9382. [CrossRef] [PubMed]

17. Ruffolo, S.A.; La Russa, M.F.; Aloise, P.; Belfiore, C.M.; Macchia, A.; Pezzino, A.; Crisci, G.M. Efficacy of nanolime in restoration procedures of salt weathered limestone rock. *Appl. Phys. A* **2014**, *114*, 753–758. [CrossRef]
18. Ruffolo, S.A.; La Russa, M.F.; Ricca, M.; Belfiore, C.M.; Macchia, A.; Comite, V.; Pezzino, A.; Crisci, G.M. New insights on the consolidation of salt weathered limestone: The case study of Modica stone. *Bull. Eng. Geol. Environ.* **2017**, *76*, 11–20. [CrossRef]
19. Matteini, M. Inorganic treatments for the consolidation and protection of stone artefacts. *Conserv. Sci. Cult. Herit.* **2008**, *8*, 13–27.
20. Pinna, D.; Salvadori, B.; Porcinai, S. Evaluation of the application conditions of artificial protection treatments on salt-laden limestones and marble. *Construct. Build. Mater.* **2011**, *25*, 2723–2732. [CrossRef]
21. Dreyfuss, T. Interactions on site between powdering porous limestone, natural salt mixtures and applied ammonium oxalate. *Herit. Sci.* **2019**, *7*, 5. [CrossRef]
22. Sassoni, E.; Naidu, S.; Scherer, G.W. The use of hydroxyapatite as a new inorganic consolidant for damaged carbonate stones. *J. Cult. Herit.* **2011**, *12*, 346–355. [CrossRef]
23. Naidu, S.; Sassoni, E.; Scherer, G.W. New treatment for corrosion-resistant coatings for marble and consolidation of limestone. In *Jardins de Pierres—Conservation of Stone in Parks, Gardens and Cemeteries*; Stefanaggi, M., Vergès-Belmin, V., Eds.; XL Print: Paris, France, 2011; pp. 289–294.
24. Dorozhkin, S.V. Calcium orthophosphates: Occurrence, properties, biomineralization, pathological calcification and biomimetic applications. *Biomatter* **2011**, *1*, 121–164. [CrossRef]
25. Sassoni, E. Hydroxyapatite and Other Calcium Phosphates for the Conservation of Cultural Heritage: A Review. *Materials* **2018**, *11*, 557. [CrossRef] [PubMed]
26. Matteini, M.; Rescic, S.; Fratini, F.; Botticelli, G. Ammonium phosphates as consolidating agents for carbonatic stone materials used in architecture and cultural heritage: Preliminary research. *Int. J. Archit. Herit.* **2011**, *5*, 717–736. [CrossRef]
27. Yang, F.W.; Liu, Y.; Zhu, Y.C.; Long, S.J.; Zuo, G.F.; Wang, C.Q.; Guo, F.; Zhang, B.J.; Jiang, S.W. Conservation of weathered historic sandstone with biomimetic apatite. *Chin. Sci. Bull.* **2012**, *57*, 2171–2176. [CrossRef]
28. Sassoni, E.; Franzoni, E.; Pigino, B.; Scherer, G.W.; Naidu, S. Consolidation of calcareous and siliceous sandstones by hydroxyapatite: Comparison with a TEOS-based consolidant. *J. Cult. Herit.* **2013**, *14*, e103–e108. [CrossRef]
29. Graziani, G.; Sassoni, E.; Franzoni, E. Consolidation of porous carbonate stones by an innovative phosphate treatment: Mechanical strengthening and physical-microstructural compatibility in comparison with TEOS-based treatments. *Herit. Sci.* **2015**, *3*, 1–6. [CrossRef]
30. Molina, E.; Rueda-Quero, L.; Benavente, D.; Burgos-Cara, A.; Ruiz-Agudo, E.; Cultrone, G. Gypsum crust as a source of calcium for the consolidation of carbonate stones using a calcium phosphate-based consolidant. *Construct. Build. Mater.* **2017**, *143*, 298–311. [CrossRef]
31. Ma, X.; Balonis, M.; Pasco, H.; Toumazou, M.; Counts, D.; Kakoulli, I. Evaluation of hydroxyapatite effects for the consolidation of a Hellenistic-Roman rock-cut chamber tomb at Athienou-Malloura in Cyprus. *Construct. Build. Mater.* **2017**, *150*, 333–344. [CrossRef]
32. Possenti, E.; Conti, C.; Gatta, G.D.; Realini, M.; Colombo, C. Diammonium hydrogen phosphate treatment on dolostone: The role of Mg in the crystallization process. *Coatings* **2019**, *9*, 169. [CrossRef]
33. Balonis-Sant, M.; Ma, X.; Kakoulli, I. Preliminary results on biomimetic methods based on soluble ammonium phosphate precursors for the consolidation of archaeological wall paintings. In *Archaeological Chemistry VIII, ACS Symposium Series*; American Chemical Society: Washington, DC, USA, 2013; Volume 1147, pp. 419–447. [CrossRef]
34. Sassoni, E.F. Lime and cement mortar consolidation by ammonium phosphate. *Construct. Build. Mater.* **2020**, *245*, 118409. [CrossRef]
35. Sassoni, E.; Graziani, G.; Franzoni, E.; Scherer, G.W. Conversion of calcium sulfate dihydrate into calcium phosphates as a route for conservation of gypsum stuccoes and sulfated marble. *Construct. Build. Mater.* **2018**, *170*, 290–301. [CrossRef]
36. Ma, X.; Pasco, H.; Balonis, M.; Kakoulli, I. Investigation of the optical, physical, and chemical interactions between diammonium hydrogen phosphate (DAP) and pigments. *Sustainability* **2019**, *11*, 3803. [CrossRef]
37. Graziani, G.; Sassoni, E.; Scherer, G.W.; Franzoni, E. Phosphate-based treatments for consolidation of salt-bearing Globigerina limestone. *IOP Conf. Ser. Mater. Sci. Eng.* **2018**, *364*, 012082. [CrossRef]

38. Sassoni, E.; Graziani, G.; Franzoni, E. An innovative phosphate-based consolidant for limestone. Part 2: Durability in comparison with ethyl silicate. *Construct. Build. Mater.* **2016**, *102*, 931–942. [CrossRef]
39. Molina, E.; Fiol, C.; Cultrone, G. Assessment of the efficacy of ethyl silicate and dibasic ammonium phosphate consolidants in improving the durability of two building sandstones from Andalusia (Spain). *Environ. Earth Sci.* **2018**, *77*, 302. [CrossRef]
40. Shekofteh, A.; Molina, M.; Rueda-Quero, L.; Arizzi, A.; Cultrone, G. The efficiency of nanolime and dibasic ammonium phosphate in the consolidation of beige limestone from the Pasargadae World Heritage Site. *Archaeol. Anthropol. Sci.* **2019**. [CrossRef]
41. Wheeler, G. Alkoxysilanes and the Consolidation of Stone. In *Research in Conservation*; The Getty Conservation Institute: Los Angeles, CA, USA, 2005.
42. Sassoni, E.; Graziani, G.; Franzoni, E. An innovative phosphate-based consolidant for limestone. Part 1: Effectiveness and compatibility in comparison with ethyl silicate. *Construct. Build. Mater.* **2016**, *102*, 918–930. [CrossRef]
43. Maravelaki-Kalaitzaki, P.; Kallithrakas-Kontos, N.; Korakaki, D.; Agioutantis, Z.; Maurigiannakis, S. Evaluation of silicon-based strengthening agents on porous limestones. *Prog. Org. Coat.* **2006**, *57*, 140–148. [CrossRef]
44. da Fonseca, B.S.; Piçarra, S.; Pinto, A.P.F.; Montemor, M.d. Polyethylene glycol oligomers as siloxane modificators in consolidation of carbonate stones. *Pure Appl. Chem.* **2016**, *88*, 1117–1128. [CrossRef]
45. Burgos-Cara, A.; Rodríguez-Navarro, C.; Ortega-Huertas, M.; Ruiz-Agudo, E. Bioinspired Alkoxysilane Conservation Treatments for Building Materials Based on Amorphous Calcium Carbonate and Oxalate Nanoparticles. *ACS Appl. Nano Mater.* **2019**, *2*, 4954–4967. [CrossRef]
46. Moropoulou, A.; Haralampopoulos, G.; Tsiourva, T.; Auger, F.; Birginie, M. Artificial weathering and non-destructive tests for the performance evaluation of consolidation materials applied on porous stones. *Mater. Struct.* **2003**, *36*, 210–217. [CrossRef]
47. Franzoni, E.; Graziani, G.; Sassoni, E. TEOS-based treatments for stone consolidation: Acceleration of hydrolysis-condensation reactions by poulticing. *J. Sol-Gel Sci. Tech.* **2015**, *74*, 398–405. [CrossRef]
48. Naidu, S.; Liu, C.; Scherer, G.W. Hydroxyapatite-based consolidant and the acceleration of hydrolysis of silicate-based consolidants. *J. Cult. Herit.* **2015**, *16*, 94–101. [CrossRef]
49. Wurster, C.M.; Munksgaard, N.; Zwart, C.; Bird, M. The biogeochemistry of insectivorous cave guano: A case study from insular Southeast Asia. *Biogeochemisty* **2015**, *124*, 163–175. [CrossRef]
50. Shahack-Gross, R.; Berna, F.; Karkanas, P.; Weiner, S. Bat guano and preservation of archaeological remains in cave sites. *J. Archaeol. Sci.* **2004**, *31*, 1259–1272. [CrossRef]
51. Naidu, S.; Scherer, G.W. Nucleation, growth and evolution of calcium phosphate films on calcite. *J. Colloid Interface Sci.* **2014**, *435*, 128–137. [CrossRef]
52. Sassoni, E.; Graziani, G.; Franzoni, E.; Scherer, G.W. Calcium phosphate coatings for marble conservation: Influence of ethanol and isopropanol addition to the precipitation medium on the coating microstructure and performance. *Corros. Sci.* **2018**, *136*, 255–267. [CrossRef]
53. Tendero, C.; Tixier, C.; Tristant, P.; Desmaison, J.; Leprince, P. Atmospheric pressure plasmas: A review. *Spectrochim. Acta B* **2006**, *61*, 2–30. [CrossRef]
54. Patelli, A.; Verga, E.; Nodari, L.; Petrillo, S.M.; Delva, A.; Ugo, P.; Scopece, P. A customised atmospheric pressure plasma jet for conservation requirements. *IOP Conf. Ser. Mater. Sci. Eng.* **2018**, *364*, 012079. [CrossRef]
55. Sandrolini, F.; Franzoni, E.; Cuppini, G. Predictive diagnostics for decayed ashlars substitution in architectural restoration in Malta. *Mater. Eng.* **2000**, *11*, 323–337.
56. *Conservation of Cultural Property -Test Methods -Determination of Water Absorption by Capillarity*; European Standard EN 15801; European Standard EN: Brussels, Belgium, 2010.
57. *Conservation of Cultural Property -Test Methods -Determination of Water Vapor Permeability (δp)*; European Standard EN 15803; European Standard EN: Brussels, Belgium, 2010.
58. Sandrolini, F.; Franzoni, E.; Sassoni, E.; Diotallevi, P.P. The contribution of urban-scale environmental monitoring to materials diagnostics: A study on the Cathedral of Modena (Italy). *J. Cult. Herit.* **2011**, *12*, 441–450. [CrossRef]

59. Sassoni, E.; Graziani, G.; Ridolfi, G.; Bignozzi, M.C.; Franzoni, E. Thermal behavior of Carrara marble after consolidation by ammonium phosphate, ammonium oxalate and ethyl silicate. *Mater. Des.* **2017**, *120*, 345–353. [CrossRef]
60. Sassoni, E.; Andreotti, S.; Scherer, G.W.; Franzoni, E.; Siegesmund, S. Bowing of marble slabs: Can the phenomenon be arrested and prevented by inorganic treatments? *Environ. Earth Sci.* **2018**, *77*, 387. [CrossRef]
61. Karampas, I.A.; Kontoyannis, C.G. Characterization of calcium phosphates mixtures. *Vib. Spectrosc.* **2013**, *64*, 126–133. [CrossRef]
62. Franzoni, E.; Sassoni, E.; Graziani, G. Brushing, poultice or immersion? The role of the application technique on the performance of a novel hydroxyapatite-based consolidating treatment for limestone. *J. Cult. Herit.* **2015**, *16*, 173–184. [CrossRef]
63. Graziani, G.; Sassoni, E.; Scherer, G.W.; Franzoni, E. Penetration depth and redistribution of an aqueous ammonium phosphate solution used for porous limestone consolidation by brushing and immersion. *Construct. Build. Mater.* **2017**, *148*, 571–578. [CrossRef]
64. Sassoni, E.; Graziani, G.; Franzoni, E. Repair of sugaring marble by ammonium phosphate: Comparison with ethyl silicate and ammonium oxalate and pilot application to historic artifact. *Mater. Des.* **2015**, *88*, 1145–1157. [CrossRef]
65. Sassoni, E.; D'Amen, E.; Roveri, N.; Scherer, G.W.; Franzoni, E. Durable self-cleaning coatings for architectural surfaces by incorporation of TiO2 nanoparticles into hydroxyapatite films. *Materials* **2018**, *11*, 177. [CrossRef]
66. Delgado Rodrigues, J.; Grossi, A. Indicators and ratings for the compatibility assessment of conservation actions. *J. Cult. Herit.* **2007**, *8*, 32–43. [CrossRef]

© 2020 by the authors. Licensee MDPI, Basel, Switzerland. This article is an open access article distributed under the terms and conditions of the Creative Commons Attribution (CC BY) license (http://creativecommons.org/licenses/by/4.0/).